Pure Appl. Chem., Vol. 74, No. 10, pp. 1871–1884, 2002.

Derivation of complete phase diagrams for ternary systems with immiscibility phenomena and solid–fluid equilibria*

V. M. Valyashko

Kurnakov Institute of General and Inorganic Chemistry, Russian Academy of Sciences, Moscow 117907, Russia

Abstract: Four main types of binary fluid-phase diagrams and available experimental data on binary systems are used as a starting point for derivation of the systematic classification of binary complete phase diagrams by the method of continuous topological transformations. This method and the classification of binary phase diagrams, containing the boundary versions of phase diagrams with ternary nonvariant points, are applied to derive the main types of fluid and complete phase diagrams for ternary systems with one volatile component and immiscibility phenomena in two constituent binary subsystems. The results gained from this analysis of derived fluid and complete phase diagrams of ternary systems are represented.

INTRODUCTION

The pioneering work of van der Waals and his school on the equation of state and the thermodynamics of mixtures at the end of the 19th and beginning of the 20th centuries laid a basis for the modern theory of heterogeneous equilibria and phase diagrams. Van der Waals and his coworkers developed the "classical approach" to phase diagram derivation, in which phase behavior of mixtures was established by investigation of the behavior of thermodynamic functions (free energy) in P–V–T–X space, which could be calculated from the equation of state. Originally, the theoretical derivation of phase diagrams was made by a topological method after the main features of a geometry of thermodynamic surfaces were obtained from limited calculations (available at that time) using the equation of state [1]. The following continuous transformations and combinations of the geometrical features of the surfaces were made topologically, as well as a derivation of topological schemes of phase diagrams from the interplay of the thermodynamic surfaces. The topological approach and the knowledge of the regularities of behavior and intersections of thermodynamic surfaces for various phases including the solid phase permitted the derivation of not only the several types of fluid phase diagram, but also the schemes of phase diagrams with participation of the solid phase [1–3].

Since the first publication of Scott and van Konynenburg in 1970 on global phase behavior of binary fluid mixtures [4], the classical approach to the derivation of phase diagrams has changed from the topological method to the analytical method. Analytical investigation of various liquid–gas equations of state [4–12] shows the same main types of fluid phase behavior for different kinds of molecular interactions and the same sequences of transformation of one type of binary phase diagram into another. Such calculations do not permit study of phase equilibria with solid phases because a general liquid–gas–solid equation of state is absent. The traditional classification of binary fluid based on the available experimental data and results of investigation the liquid–gas equations of state contains seven

*Lecture presented at the 10th International Symposium on Solubility Phenomena, Varna, Bulgaria, 22–26 July 2002. Other lectures are published in this issue, pp. 1785–1920.

types of fluid phase behavior [4,5]. This classification includes four different types (I, V, VI, and VII) of fluid phase behavior, where the intersections of critical curves and immiscibility regions with a crystallization surface are absent. Three other types (II, III, and IV) are the result of solid phase interference in immiscibility and critical equilibria of types V, VI, and VII.

For rigorous derivation of the complete phase diagrams, which describe not only fluid equilibria but also all the equilibria with solid phase, simultaneous investigation of two equations of state (for liquid–gas and for solid phases) should be made.

Another possibility is to turn back to the topological method at the level of topological schemes of phase diagram rather than on the level of thermodynamic surfaces. Modern knowledge of phase diagrams construction permits not only classification of the main types of diagrams but finding some regularities of transformation of one type of phase diagram into another.

The fundamental idea of continuous transitions between the various forms of heterogeneous fluid equilibria and types of fluid phase diagrams was formulated by Schneider [13,14] and confirmed by systematic investigations of "families" of binary systems when one component is the same, while the other is altered in size, shape, and/or polarity. It has also been proven by the studies of ternary systems where the quasi-binary cross-sections show a continuous transformation of fluid phase behavior.

Theoretical calculation of fluid phase diagrams also shows that each diagram transforms continuously into another when the model parameters are changed. Special boundary versions of phase diagrams arise in the process of transformation. The curves in the global phase diagrams divide the diagram field into domains of different phase behavior and correspond to so-called "boundary versions" of the fluid phase diagram [4–12]. Such boundary versions have properties of both neighboring types but cannot be realized since, in violation of the Phase Rule, they contain equilibria, which are possible only in ternary or more complicated systems.

A similar approach, which considers the diagrams as stages in the continuous process of topological transformation, was applied to the complete phase diagram [15,16], which describes any equilibria with liquid, gas, and/or solid phases in a wide range of temperature and pressure.

The main objectives of this paper are to demonstrate the last version of systematic classification for binary complete phase diagrams obtained by the method of continuous topological transformation and to show how this method and the systematic classification of binary diagrams can be used for derivation of complete phase diagrams of ternary systems containing one volatile component and immiscibility phenomena in two binary subsystems.

CLASSIFICATION OF COMPLETE PHASE DIAGRAMS OF BINARY SYSTEMS

The method of continuous topological transformation is based on the premise that each type (or topological scheme) of phase diagram can be continuously transformed into another type through the boundary version of that phase diagram, which has the properties of both neighboring types and contains the equilibria possible only in the systems with the higher numbers of components. In the case of transformation of binary fluid equilibria, the boundary versions can be borrowed from the global phase diagrams of binary fluid mixtures. Modifications of stable fluid phase equilibria in presence of a solid phase do not change the type and topological scheme of fluid phase and originate in the boundary versions of phase diagram with nonvariant ternary critical points where the solid phase takes part in equilibria. As a result of such modification, a part of fluid equilibria (for instance, the parts of immiscibility regions and/or critical curves) is suppressed by solidification of the nonvolatile component and transforms into the metastable equilibria.

Some types of binary complete phase diagrams can be found from available experimental data, and these types were used as a starting point for derivation of systematic classification. A systematic classification that includes both known and new types of complete phase diagrams, which fill the empty places in the chain of continuous transformation and are separated by the boundary versions, are shown in Fig. 1.

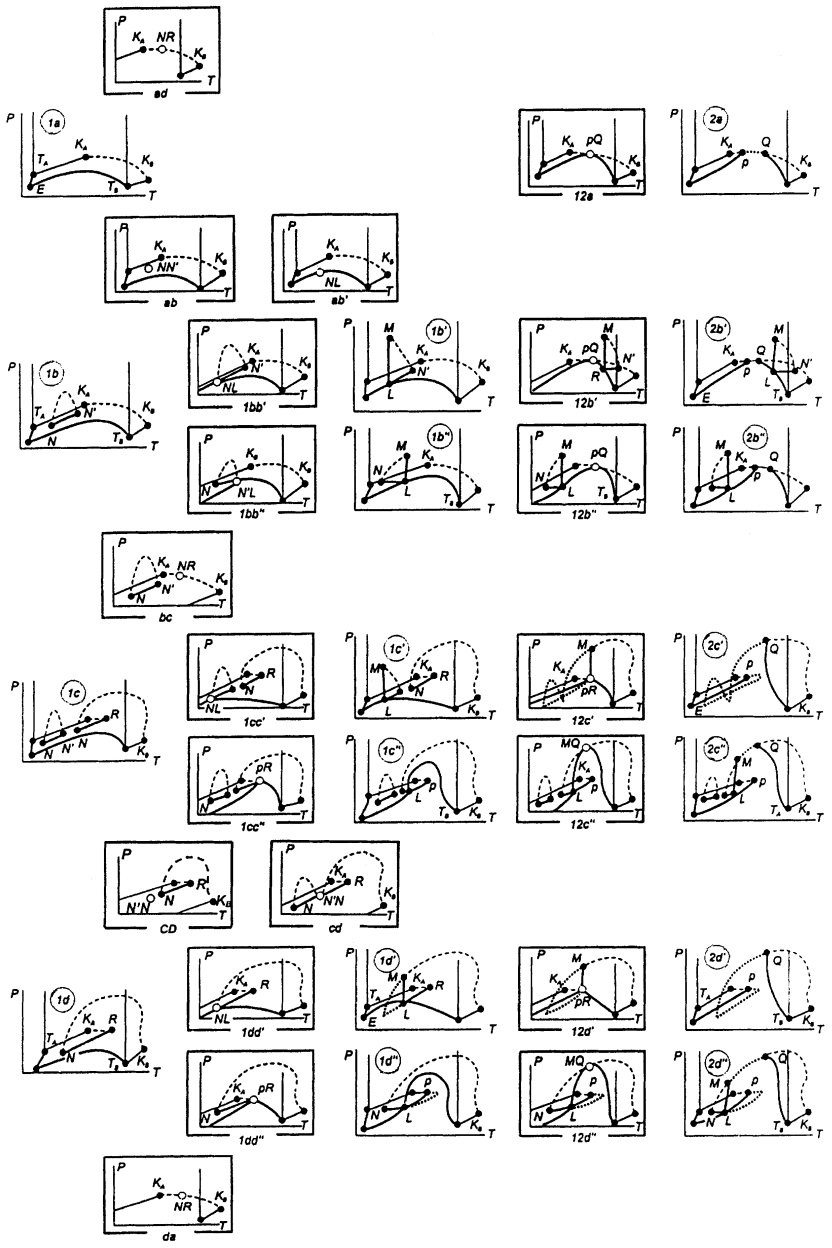

Fig. 1 Systematic classification of binary complete phase diagrams (P-T projections).

Boundary versions of phase diagram are shown in frames. Solid circles are nonvariant points in one- and two-component systems [T_A, T_B and K_A, K_B – triple (L–G–S) and critical (L = G) points of pure components A and B, eutectic point E (L–G–S_A–S_B), L (L_1–L_2–G–S_B); critical end-points: N (N′) (L_1 = L_2–G), R (L_1 = G–L_2), p (L = G–S), Q (L = G–S or L_1 = L_2–S), M (L_1 = L_2–S)]; open dots are the nonvariant equilibria of ternary systems [NL (N′L) (L_1 = L_2–G–S), pR (L_1 = G–L_2–S), double critical end-points N′N (L_1 = L_2–G), pQ (L = G–S), MQ (L_1 = L_2–S); tricritical point NR (L_1 = L_2 = G)] in the boundary versions of phase diagram (in frames). Thin lines are the monovariant equilibria L–G and L–S of pure components A and B; dashed lines are the critical curves L = G and L_1 = L_2; heavy lines are the monovariant curves (noncritical) of binary system; dotted lines are the metastable parts of monovariant curves in binary systems.

To facilitate a systematic and simplified approach to construction of complete phase diagrams and simultaneously to bring the topological schemes as close as possible to the description of phase equilibria in high-temperature water–salt systems, the following limitations for the main types of binary complete phase diagrams are necessary [15,16]:

1. The melting temperature of the pure nonvolatile (salt) component is higher than the critical temperature of the volatile component (water).
2. Solid-phase transformations (polymorphism, formation of solid solutions and compounds, and azeotropy in liquid–gas equilibria) are all absent, and solid–fluid equilibria have a eutectic nature.
3. Liquid immiscibility is terminated by the critical region ($L_1 = L_2$) at high pressures and cannot be represented by more than two separated immiscibility regions of different types.
4. All geometric elements of phase diagrams, their reactions, and shapes (but not the combinations of these elements) can be illustrated by existing experimental examples.

Each diagram is labeled with a number (**1** or **2**) followed by a type (**a**, **b**, **c**, or **d**) of fluid phase behavior. Titles of boundary versions of the complete phase diagram contain two letters (for examples, **ab**, **CD**, **1bb′**, **1dd″**) or two numbers (**12a**, **12d″**) according to the neighboring types, which transform one into another.

The numbers (**1**, **2**), reflecting both the features of solid–fluid equilibria and the traditional division of the complete phase diagram, fall into two types. The first type (type **1**) has no intersection of solubility (L–G–S) and critical (L = G) curves. Type p-Q (or type **2**), the second type, has intersections of solubility and critical curves at two critical end-points «p» and «Q» (L = G–S) [2,15–19]. The systems of type **1** have a positive temperature coefficient of solubility (t.c.s.) in the three-phase equilibrium (L–G–S) and an uninterrupted solubility curve at supercritical temperatures. Type **2** is characterized by a negative t.c.s. in the subcritical equilibrium region (L–G–S), critical phenomena in saturated solutions (L = G–S) (critical end-points "p" and "Q"), and supercritical fluid equilibria in the temperature range between the critical end-points "p" and "Q". A distinguishing feature of supercritical fluid equilibria is an occurrence of only one fluid phase (with or without equilibrium solid phase), regardless of pressure variations. A transition from the gas-like state of fluid at low pressures/densities to the liquid-like fluid at high pressures/densities takes place continuously without the two-phase fluid equilibrium and density jump at any compression.

Phase equilibria in types **1** and **2** may be complicated by the immiscibility of liquid phases taking place both in stable and metastable conditions.

The systematic classification in Fig. 1 consists of four rows (**a**, **b**, **c**, and **d**) of the diagrams, corresponding to four main types of fluid phase behavior.

Complete phase diagrams in row **a** are characterized by a fluid phase behavior without liquid–liquid immiscibility phenomena. A limited immiscibility region is a permanent element of complete phase diagrams of the row **b**. Two three-phase immiscibility regions L_1–L_2–G of different nature are the constituents of complete phase diagrams in the row **c**. Fluid phase behavior of type **d** can be found in any complete phase diagrams of row **d**.

Three horizontal rows (**b**, **c**, and **d**) consist of two lines of phase diagrams because there are the experimental examples for phase diagrams of both lines in row **d**. Although the phase diagrams of lines **b″** and **c″** (derived by the same manner as the diagrams in the line **d″**) were not encountered experimentally, there is no reason to reject these topological schemes as the possible types of binary phase behavior.

There are three columns (right, central, and left) of complete phase diagrams (P-T diagrams without frames) separated by two vertical columns of boundary versions (P-T diagrams in frames) in Fig. 1. The complete phase diagrams, which show four main types of fluid phase behavior (types **a**, **b**, **c**, and **d** in our classification or types I, V, VI, and VII according to traditional classification of binary fluid phase behavior [4,5]) and lack critical phenomena in solid-saturated solutions, are found in the left column (types **1a**, **1b**, **1c**, **1d** of complete phase diagram). The central and right columns contain dia-

grams with nonvariant points where critical phenomena occur in equilibrium with a solid phase. So-called "supercritical fluid–solid equilibria" are absent in the diagrams from central column (types **1b′**, **1b″**, **1c′**, **1c″**, **1d′**, **1d″**), but they appear in the systems of type **2** described by the diagrams of types **2a**, **2b′**, **2b″**, **2c′**, **2c″**, **2d′**, and **2d″** from the right column.

Supercritical fluid–solid equilibria, where a transition from gas-like fluids to liquid-like ones occur continuously without the two-phase equilibrium and density jump, occur in systems where the critical temperature of the volatile component is lower than the melting temperature of nonvolatile one. Such phase behavior was observed in systems of gases (Ne–Ar, H_2–CO_2, H_2–CH_4, etc. [20]), organics (CH_4–cyclohexane, CH_4–*n*-octane, ethylene–naphthalene, ethylene–anthracene, etc. [21], CH_4–diamondoids [22]), and aqueous electrolytes/inorganic compounds (H_2O–SiO_2, H_2O–Na_2CO_3, H_2O–Li_2SO_4, H_2O–K_2SO_4, H_2O–$BaCl_2$, etc. [15,19]). It is important to note that most of type **2** systems where high-temperature supercritical equilibria were studied in detail are complicated by metastable immiscibility regions and belong to type **2d′** or **2d″**. Only CH_4–diamondoids systems show type **2a** phase behavior without immiscibility phenomena [22].

Diagrams from Fig. 1 included in boxes are the boundary versions of a binary phase diagram. They contain the special points representing nonvariant equilibria in ternary systems and demonstrate continuity of topological transformation of one binary type of a complete phase diagram into another.

There are two boundary versions between rows **a** and **b** and between rows **c** and **d**. In the first case, the boundary version **ab** appears at the transition of type **1a** into type **1b**. The boundary version **ab′** takes place in the transformation **1a**–**1ab′**–**1b′**, **1a**–**1ab′**–**1b″**, **2a**–**2ab′**–**2b′**, **2a**–**2ab′**–**2b″**. In the second case, the boundary version **cd** may take part in a continuous topological transformation of any phase diagrams in rows **c** and **d**. However, the global phase diagrams of binary fluid mixtures [8,9] show also another way of continuous transformation for phase diagrams of types **1c–1d** (possible for **1c″**–**1d″**, **2c″**–**2d″**) through the boundary version **CD**.

All seven types of fluid phase diagrams introduced by [4,5] can be easily found as a part of the following complete phase diagrams of type **1** (placed in the left and central columns): type I (fluid phase diagram) = type **1a** (complete phase diagram), type II = type **1b′**, type III = type **1d′**, type IV = type **1c′**, type V = type **1d**, type VI = type **1b**, type VII = type **1c**.

Seven of ten types of complete phase diagram from the left and central columns (type **1**) have the experimental examples. Here are the few examples of each type: type **1a** (CH_4–propane, CO_2–cyclohexane, NH_3–H_2O, H_2O–NaCl [13,14]); type **1b** (2-butanol–H_2O, 2-methylpyridine–D_2O, 2-butanone–H_2O [13,14]); type **1b′** (CO_2–octane [13,14], H_2O–HgI_2 [23,24]); type **1c′** (CH_4–1-hexene, CH_4–2-methyl-1-pentene, CH_4–3.3-dimethylpentane, CH_4–2.3-dimethyl-1-buten [13,14]); type **1d** (CO_2–nitrobenzene, CH_4–hexane [13,14], H_2O–UO_2SO_4 [25,26], H_2O–$Na_2B_4O_7$ [27]); type **1d′** (CH_4–methylcyclopentane, CO_2–hexadecane, CO_2–H_2O [13,14], H_2O–$PbBr_2$, H_2O–PbI_2 [23,24]); type **1d″** (? H_2O–UO_2F_2 [28]).

Some types of complete phase diagrams, shown in Fig. 1, have not been experimentally documented (**1b″**, **2b′**, **2b″**, **1c**, **1c″**, **2c′**, **2c″**).

TERNARY SYSTEMS

As well as in the case of binary systems, a diversity of complete phase diagrams of ternary systems depends both on the variety of the main types of ternary fluid phase behavior and on the possible versions of solid–fluid equilibria, which appear as a result of intersection of fluid phase equilibria with the crystallization surfaces. However, the abundance of ternary types is much greater than the binary. There are 39 main types (classes) of fluid phase diagrams for ternary systems, where one of the binary subsystems belongs to type **1a** and another two binary subsystems with volatile component are complicated by immiscibility phenomena [29] and more than 130 distinct classes of complete ternary phase diagrams of such ternary systems. Therefore, only a general observation of our approach to the theoretical derivation of ternary phase diagrams and some examples of ternary complete phase diagrams will be

given after a brief discussion of graphical representation of ternary phase diagrams in the following sections.

Graphical representation of ternary phase diagrams

The most correct and complete representations of four-dimensional ternary phase diagrams are given by the isothermal or isobaric triangle prisms (isothermal or isobaric cross-sections of ternary phase diagrams) where the vertical axis is either the pressure or temperature, and the triangle prism base represents the ternary concentrations. All types of phase behavior can be described by the sets of such isothermal or isobaric prisms, although these phase diagrams become very difficult to interpret due to enrichment of points, curves, and surfaces.

Two-dimensional P-T projection or triangle prism of T-X and P-X projections can be used for correct representations of mono- and nonvariant equilibria over wide ranges of temperature and pressure. Sometimes, the three-dimensional T-X or P-X projection can be represented as a triangle of ternary concentrations with a set of isotherms or isobars that describe the phase behavior in a range of temperature or pressure.

Figure 2 is an example of three-dimensional T-X projection for ternary system with one volatile component (A) and two nonvolatile components (B and C) forming continuous solid solutions. Binary subsystems A-C and C-B belong to the type **1a**, whereas the system A-B belongs to the type **1b′**. The ternary phase diagram shows the surfaces of liquid phase compositions in equilibria L–G–S (shady surface T_AE_{AB}L–NL–L–$T_BT_CE_{AC}T_A$ in Fig. 2) and L_1–L_2–G (N–L–NL–L–N) and the critical surfaces L = G (shady surface $K_AK_BK_C$) and $L_1 = L_2$ (N–M–NL–M). The cross-sections at constant ratios of nonvolatile components (B/C) are shown on the surfaces. These sections depict the continuously transforming T-X diagrams of quasi-binary subsystems with permanent volatile component A and nonvolatile component represented by a continuously changed mixture of B and C. The stable and metastable parts of three-phase immiscibility region L_1–L_2–G shrink with increasing of C concentration in the mixture and end in the nonvariant critical point NL ($L_1 = L_2$–G–S).

The P-T projections do not carry information on the composition of the equilibrium phases. An attempt has been made to use a four-angle prism with P, T, and X* as axes for a representation of divariant critical surfaces and monovariant critical curves in the ternary systems as a continuous set of quasi-binary P-T sections at constant X* [30,31]. The X* axis denotes relative amounts of the nonvolatile components $X^* = X_2/(X_2 + X_3)$ in ternary solutions. However, in such diagrams, the representation of the critical point of a volatile component and equilibria in the vicinity is not absolutely correct, because the critical point of volatile component is displayed as a straight line. To avoid this uncertainty and to circumvent an application of three-dimensional figures, which are usually complicated for perception, the two-dimensional T-X* projections can be used for presentation of the ternary equilibria between phases enriched with nonvolatile components. As one can see from Fig. 2, the T-X* projection (heavy curves on the T-X* plane CBK_BK_C) is obtained from the three-dimensional T-X diagram and contains only binary and ternary nonvariant points and ternary monovariant curves. Nonvariant points of pure components can be omitted on the T-X* projection because they are placed on the ordinates and do not take part in a formation of ternary monovariant curves.

It is assumed that the vapor (gas) phase of the equilibria $L_1 = L_2$–G and L_1–L_2–G–S as well as the critical phase of the equilibrium L_1 = G–L_2 is almost pure volatile component and does not plot on the T-X* projection. Therefore, the composition (X*) of the critical phase ($L_1 = L_2$) in the first case, one of the liquid phases (or both equilibrium liquids if they have the same B/C ratio) in the equilibrium L_1–L_2–G–S and the noncritical phase (L_2) in the critical equilibrium L_1 = G–L_2 shows the position of the monovariant equilibria on the T-X* diagram.

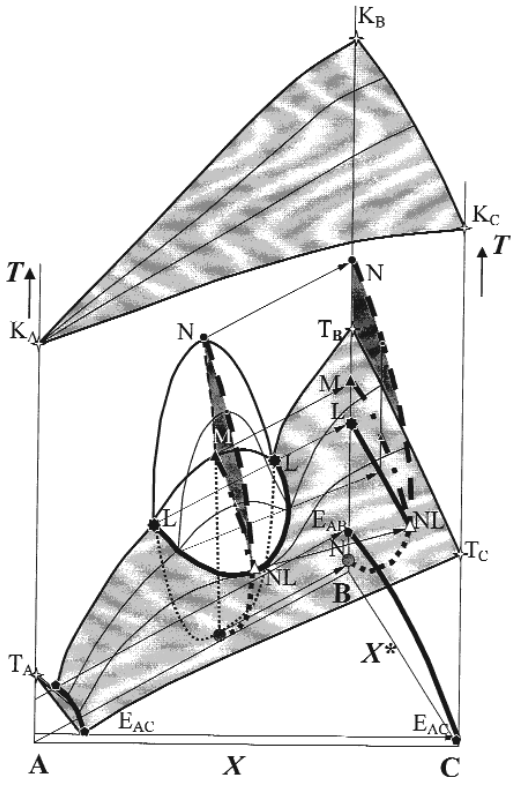

Fig. 2 Prismatic representation of T-X projection for complete phase diagram of ternary system A-B-C (A is volatile component) and T-X* projection of ternary monovariant curves on the plane CBK_BK_C.

Points T_A, T_B, T_C and K_A, K_B, K_C are the triple and critical points of pure components; points E_{AB}, E_{AC}, L, M, N are the compositions of liquid and critical phases in binary nonvariant equilibria L–G–S_A–S_B, L–G–S_A–S_C, L_1–L_2–G–S, L_1 = L_2–S, L_1 = L_2–G; point NL is the composition of critical phase in ternary nonvariant equilibrium L_1 = L_2–G–S. Solid lines are the composition of liquid and critical phases in binary monovariant equilibria L–G–S, L_1–L_2–G, L_1–L_2–S, and L = G; thin lines are the compositions of liquid and critical phases at constant ratio B/C in ternary equilibria L–G–S, L_1–L_2–G, L_1–L_2–S and L = G; dashed lines are the composition of critical phase in binary monovariant equilibrium L_1 = L_2 and ternary monovariant equilibrium L_1 = L_2–G; dot-dashed line is the composition of critical phase in ternary monovariant equilibrium L_1 = L_2–S; dotted lines are the metastable parts of monovariant curves in binary equilibria L_1–L_2–G, L_1 = L_2 and in ternary equilibrium L_1 = L_2–G; heavy lines are the compositions of liquid and critical phases in ternary monovariant equilibria L_1–L_2–G–S, L–G–S_A–S_{BC}, L_1 = L_2–G and L_1 = L_2–S. Shaded surfaces are the compositions of liquid phase in ternary equilibrium L–G–S (T_AE_{AB}L–NL–L–$T_BT_CE_{AC}$) and the compositions of critical phases in ternary equilibria L = G ($K_AK_BK_C$) and L_1 = L_2 (N–M–NL). X* is the relative amounts of the nonvolatile components (B, C) in ternary solutions [$X^* = X_B/(X_B + X_C)$].

Derivation of ternary phase diagrams with the use of systematic classification of binary phase diagrams

If the phase behavior of the constituent binary subsystems is known, the task of constructing a topological scheme for a ternary system translates into the finding of new nonvariant equilibria. These equilibria result from the intersection of monovariant curves originated at nonvariant points of the constituent binary subsystems. While passing from one binary subsystem to another, the phase diagrams of the binary subsystems must undergo continuous topological transformations in the three-component

region of composition. This process may be imagined as a continuous phase diagram transformation of quasi-binary sections of the ternary system with a constant volatile component (water in the case of water–salt systems) and a continuously changing nonvolatile component (salt component in the case of water–salt systems) from one nonvolatile component to another. This constitutes so-called "quasi-binary approach" to the ternary phase equilibria.

Representation of three-component systems as a set of quasi-binary cross-sections is not quite rigorous for most real ternary mixtures. However, if we intend to study the phase behavior on the level of topological schemes, the sequence of binary phase diagrams of quasi-binary sections (including the sections through the ternary nonvariant points) gives an exhaustive description of possible phase equilibria and phase transformations in ternary systems.

If the phase diagrams of the binary subsystems are present in Fig. 1, then all the steps of the topological transformation between these diagrams are also shown on the same figure as a set of complete phase diagrams corresponding to the quasi-binary sections. Such sets include the boundary versions of phase diagrams, which show ternary nonvariant points that should appear in the studied three-component systems. For example, the sequence of quasi-binary sections of ternary phase diagram for the systems with binary subsystems of types **1b′** and **1d′** could be the following: **1b′⇔1b′a⇔1a⇔1ad⇔1d⇔1dd′⇔1d′**, according to Fig. 1. Such phase behavior was found experimentally in the system HgI_2–PbI_2–H_2O [24]. However, as shown by [32] and from Fig. 1, the same class of ternary system (**1b′–1d′–1a**) can have another type of phase behavior **1b′⇔1b′c′⇔1c′⇔1c′d′⇔1d′** if both immiscibility regions are joined. Another example of various versions of ternary phase diagrams for one class of ternary system was found for ternary systems SiO_2–$Na_2Si_2O_5$–H_2O and $Na_2Si_2O_5$–Na_2SiO_3–H_2O [33] and is evident from Fig. 1. The binary water–salt subsystems belong to type **2d′** in both cases, but the ternary phase behavior is different and corresponds to the following sequences of binary and quasi-binary sections **2d′⇔12d′⇔1d′⇔1dd′⇔1d⇔1dd′⇔1d′⇔12d′⇔2d′** and **2d′⇔2d′**, respectively.

Harnessing the contents of Fig. 1 opens an ample opportunity for derivation of possible versions of complete phase diagram for ternary systems when the phase diagrams of binary subsystems are known. However, all the limitations accepted for the systematic classification of binary complete phase diagrams are extended to the ternary phase diagrams, which may have negative consequences. For instance, careful analysis of fluid multiphase equilibria in ternary mixture [32] shows that the phase diagrams of some quasi-binary sections can have three separated three-phase immiscibility regions of different types and two separated three-phase equilibrium L_1–L_2–G of the same type. The topological schemes of such phase diagrams are absent in the systematic classification (Fig. 1) due to the accepted limitations, hence, ternary phase diagrams with such quasi-binary sections can not be derived by this method.

Derivation of fluid and complete ternary phase diagrams

A more systematic approach to the global phase behavior of ternary systems should start from a derivation of the main types of ternary fluid phase diagrams and following consideration of how these phase diagrams are modified by the presence of the solid phase of the nonvolatile components. All possible versions of fluid and complete phase diagrams for ternary systems, as well as their classifications, is too complex a topic for discussion here. Therefore, this section contains only a brief description of the general approach to derivation of ternary phase diagrams, and an outline of some results that were gained from the analysis of fluid and complete phase diagrams for the ternary systems with one volatile and two nonvolatile components where two binary subsystems with volatile component are complicated by immiscibility phenomena and the third binary subsystem belongs to type **1a.**

Six classes of ternary fluid mixtures

As in binary systems, the main types of fluid phase diagram of ternary mixtures should not have an intersection of critical curves and immiscibility regions with a crystallization surface. Therefore, a combination of four main types (**a**–**d**) of fluid phase diagrams or types **1a**, **1b**, **1c**, and **1d** of complete phase diagrams constituting binary subsystems can result in all major classes of ternary fluid systems.

There are six major classes of ternary fluid mixtures with one volatile component and immiscibility phenomena in binary subsystems that can be referred to as ternary class **I** with the following combination of constituting binary subsystems (**1a**–**1b**–**1b**); ternary class **II**: (**1a**–**1c**–**1c**); ternary class **III**: (**1a**–**1d**–**1d**); ternary class **IV**: (**1a**–**1b**–**1d**); ternary class **V**: (**1a**–**1b**–**1c**); and ternary class **VI**: (**1a**–**1c**–**1d**) [29].

Several types of fluid phase behavior and various versions of fluid phase diagrams can characterize each class of ternary mixtures. Therefore, a designation of each version of a fluid phase diagram [29] contains a Greek letter [**α β**, **γ**, **δ**, **ε** with or without superscripts (′ and ″, ^{0})] besides a Roman numeral (**I**–**VI**). The Greek letter indicates the version of an interaction of the monovariant curves in the given class of ternary system.

It was assumed in the derivation of phase diagrams by the method of continuous topological transformation that the immiscibility regions, which are spreading from two binary subsystems, can either merge in the three-component range of composition or be separated by a miscibility region. The later case is especially important since it illustrates the phase transformations in another classes of ternary systems, where only one of the constituent binary subsystems with volatile component is complicated by liquid–liquid immiscibility: (**1a**–**1b**–**1a**), (**1a**–**1c**–**1a**), (**1a**–**1d**–**1a**).

The following are general regularities of fluid phase behavior in ternary mixtures summarized after analyzing the main types of fluid phase diagrams:

1. The immiscibility region of type **b** or **d** spreading from the binary subsystems can be terminated by one nonvariant point in ternary systems, whereas disappearance of the immiscibility region of type **c** takes place only after transformation into immiscibility region of types **b** or **d**. The end-point of the immiscibility region of type **b** is the double critical end-point (DCEP) N′N ($L_1 = L_2$–G). The spreading immiscibility region of type **d** ends in the tricritical point (TCP) RN ($L_1 = L_2 = G$). Transformation of the immiscibility region of type **c** into types **b** or **d** occurs through the TCP NR ($L_1 = L_2 = G$) or the DCEP N′N ($L_1 = L_2$–G), respectively.
2. The occurrence of two-phase holes L–G (completely bounded by a closed-loop critical curve $L_1 = L_2$–G) in the three-phase immiscibility region L_1–L_2–G bounded by a critical curve $L_1 = G$–L_2 from the high-temperature side was established experimentally for ternary systems with binary subsystems of type **d** [32]. It was assumed [29] that the occurrence of two-phase holes in the immiscibility region of such nature is a usual phenomenon for ternary mixtures with binary subsystems of type **c**. It is also possible that the two-phase hole L–G may appear in ternary three-phase immiscibility region that spreads from the binary subsystems of type **b** and bounded by two critical curves $L_1 = L_2$–G. However, the last versions of ternary fluid phase diagrams were not included in 39 main types described in [29].
3. Quasi-binary cross-sections of ternary systems with binary subsystems of type **c** (in the case of two-phase hole, in particular) can contain two separated immiscibility regions of type **b** or two immiscibility regions of type **b** and the third immiscibility region of type **d**. These types of binary fluid phase diagrams cannot be found on Fig. 1 due to the accepted limitations. However, they were obtained by calculation [5] and can be derived by the method of topological transformation if the mentioned limitation is omitted.
4. Ternary critical curves $L_1 = L_2$–G joining the binary critical end-points N pass through the double critical end-point (DCEP) N′N ($L_1 = L_2$–G) if the points N belong to one binary subsystem. In fact, two critical curves $L_1 = L_2$–G starting in binary critical end-points N of the same binary subsystems meet in DCEP. Ternary critical curve $L_1 = L_2$–G joining the critical end-points N of

various binary subsystems does not have the DCEP as well as the critical curve $L_1 = G–L_2$ connected the critical end-points R of various binary subsystems also does not have any ternary nonvariant point.

DCEP N′N appears on the critical curve $L_1 = L_2–G$ which intersects with another critical curve $L_1 = G–L_2$ in the tricritical point (TCP) NR ($L_1 = L_2 = G$) when these critical curves originate in different binary subsystems. If both critical curves of different nature start from the same binary subsystem and are intersected in TCP, the critical curve $L_1 = L_2–G$ does not have DCEP.

Two DCEP are located on the closed-loop critical curve $L_1 = L_2–G$ bounded a two-phase hole L–G in three-phase immiscibility region at extreme contents of nonvolatile components. Two TCPs appear in ternary system as a result of intersection of closed-loop critical curve $L_1 = L_2–G$ with the critical curve $L_1 = G–L_2$.

5. A continuous topological transformation of one topological type of ternary fluid phase diagram into another in the frame of one ternary class is carried out by merging together the ternary nonvariant points and by tangency of one monovariant curve to another in accordance with the rules formulated in [29].

Complete phase diagrams

Until the equilibrium L–G–S intersects the three-phase immiscibility region $L_1–L_2–G$, the stable fluid phase equilibria are not changed and correspond to the main types of fluid phase diagram. An appearance of equilibrium $L_1–L_2–G–S$ (the nonvariant point L in binary systems and the monovariant curve in ternary system) leads to transition of a part of immiscibility region into metastable conditions. An increase in temperature of solid phase interference in immiscibility and critical equilibria increases the metastable part of immiscibility region and initiates an appearance of supercritical fluid equilibria and a transition of binary or quasi-binary phase diagrams from type **1** to type **2**.

Figure 3 shows several examples of ternary complete phase diagrams represented as five T-X* projections of ternary phase diagrams for each of six ternary classes **I**–**VI**.

In order to simplify the T-X* projections of complete phase diagrams the following additional assumptions and limitations are accepted.

1. Solid phases of nonvolatile components form a continuous solid solution in binary and ternary systems. In addition, the polymorphism and formation of new compounds are absent. The assumptions do not change the limitations concerning the binary systems with volatile and nonvolatile components. However, they help to avoid the monovariant and nonvariant equilibria with two solid phases of nonvolatile components ($L–G–S_B–S_C$) in Figs. 2 and 3.
2. Equilibria with solid phases of volatile and nonvolatile components [eutectic points ($L–G–S_A–S_B$; $L–G–S_A–S_C$) and eutonic curves ($L–G–S_A–S_{BC}$)], which take place at low temperatures and do not interact with critical or immiscibility equilibria, are not plotted on T-X* projections of complete phase diagram (Fig. 3). However these equilibria (points E_{AB}, E_{AC}, curve $E_{AB}E_{AC}$) are shown both on triangle prism of T-X projection and on the plane of T-X* projection in Fig. 2.
3. If temperatures of binary nonvariant points L ($L_1–L_2–G–S$) and M ($L_1 = L_2–S$) are the same (Fig. 1), therefore, they are shown as one point (eight-pointed star) on T-X* schemes in Fig. 3. Ternary monovariant curves $L_1–L_2–G–S$ and $L_1 = L_2–S$ starting in these points and ending in the ternary nonvariant point LN ($L_1 = L_2–G–S$) coincide and are shown as a double line in Fig. 3. These assumptions are irrelevant to Fig. 2 where the temperature of point M is higher than that of point L and corresponding ternary monovariant curves are intersected only in nonvariant point LN.

A designation of each scheme of T-X* projection in Fig. 3 contains an indication of the main type of ternary fluid phase behavior (Roman numeral with Greek letter) and the Arabic numeral corresponding to the place in the row of the figure. As mentioned above, the equilibria with solid phase do not

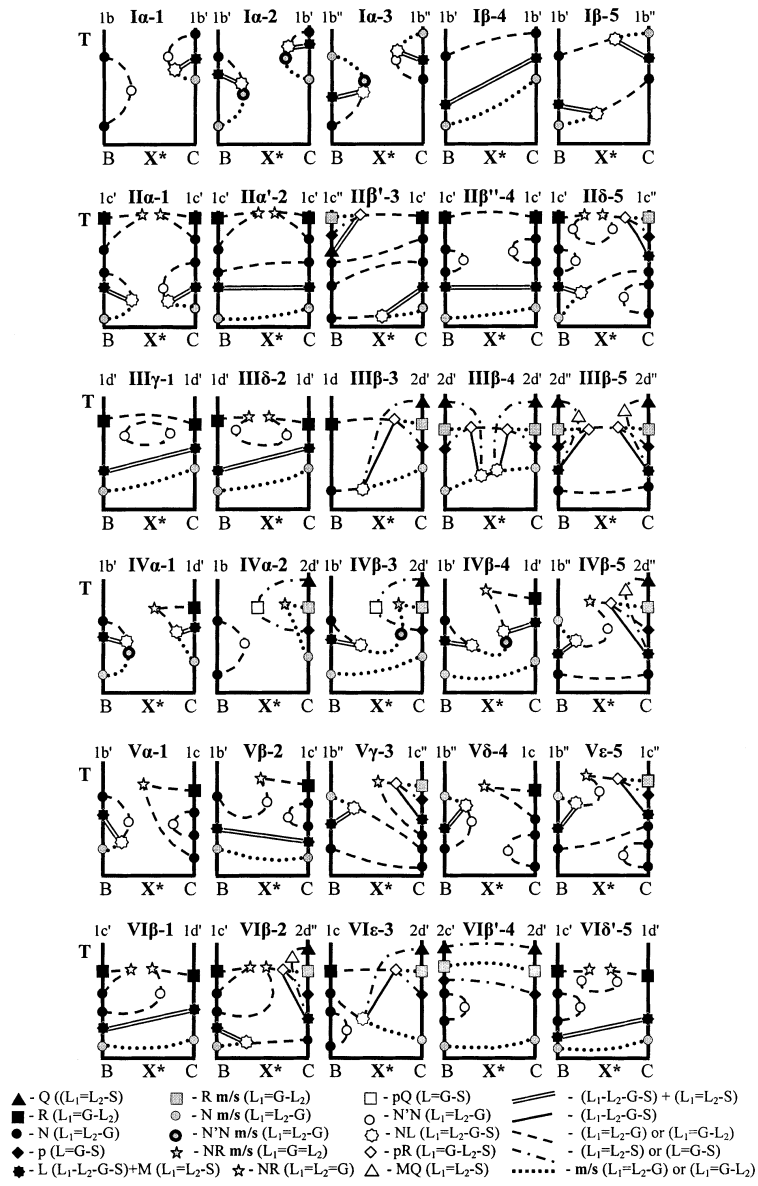

Fig. 3 T-X* projections (schemes) of some ternary complete phase diagrams for ternary systems with one volatile component and immiscibility phenomena in two binary subsystems.

Solid triangles, circles, diamonds, eight-pointed stars and squares are the binary nonvariant points Q (L_1 = L_2–S), N (L_1 = L_2–G), p (L = G–S), L (L_1–L_2–G–S) + M (L_1 = L_2–S) and R (L_1 = G–L_2). Nonvariant binary point M (L_1 = L_2–S) coincides with point L (L_1–L_2–G–S) on T-X* graph. Open triangles, eight-pointed stars, circles, five-pointed stars, squares, and diamonds are the ternary nonvariant points MQ (L_1 = L_2–S), NL (L_1 = L_2–G–S), N′N (L_1 = L_2–G), NR (L_1 = L_2 = G), pQ (L = G–S) and pR (L_1 = G–L_2–S). Shaded circles and squares in binary systems are the metastable points N (L_1 = L_2–G) and R (L_1 = G–L_2); shaded circles and stars in ternary systems are the metastable points N′N (L_1 = L_2–G) and NR (L_1 = L_2 = G). Dashed lines are the monovariant critical curves L_1 = L_2–G and L_1 = G–L_2; dot-dashed lines are the monovariant critical curves L_1 = L_2–S and L = G–S; solid lines are the monovariant curves L_1–L_2–G–S; double lines are the coincided monovariant curves L_1–L_2–G–S and L_1 = L_2–S; dotted lines are the metastable parts of critical curves L_1 = L_2–G and L_1 = G–L_2 in ternary systems. X* is the relative amounts of the nonvolatile components (B, C) in ternary solutions [$X^* = X_B/(X_B + X_C)$].

change the main type of fluid phase behavior in ternary mixture but only transform a part of fluid phase equilibria into metastable conditions. The metastable parts of such monovariant curves are shown by the dotted lines, and the metastable nonvariant points are designated by shaded marks of the same form as the stable ones. So the T-X* schemes in Fig. 3 show not only the projections of complete phase diagrams, but also the main types of ternary fluid phase diagrams that were used for derivation.

The following regularities of phase behavior in ternary systems can be formulated from the analysis of derived ternary complete phase diagrams:

1. If the immiscibility region originates in the binary subsystem of type **1b′**, **1c′**, or **1d′** (the subsystems with immiscibility phenomena in solid saturated solutions) and ends in ternary solutions, the monovariant curve L_1–L_2–G–S, starting in binary nonvariant point L, is located at temperature range below the temperature of point L and terminated by ternary nonvariant point LN ($L_1 = L_2$–G–S) as a result of intersection with ternary monovariant critical curves $L_1 = L_2$–G and $L_1 = L_2$–S, originating in binary critical end-points N and M, respectively. The low-temperature part of immiscibility region located on the T-X* projections below the monovariant curve L–LN (L_1–L_2–G–S) is metastable (Fig. 3).

   The monovariant curve L_1–L_2–G–S originated in binary subsystem of types **1b″**, **1c″**, or **1d″** is terminated by ternary critical point LN (in the case of type **1b″**) or by ternary critical point pR (L_1 = G–L_2–S) (in the cases of types **1c″** or **1d″**). However, in this case, the temperature of points LN or pR is higher than that in binary point L and the high-temperature part of three-phase immiscibility region is metastable in the range of composition (X*) from binary subsystem to ternary critical point LN or pR.

   Theoretical analysis of ternary complete phase diagrams shows that the immiscibility region originated in the binary subsystem of types **1b′** or **1b″** can disappear not only in ternary solid saturated solutions (in nonvariant point LN) (see T-X* schemes **Iα-2**, **Iα-3**, **IVα-1** in Fig. 3), but also in unsaturated solutions in DCEP N′N ($L_1 = L_2$–G) (see T-X* schemes **Iα-1**, **IIα-1**, **Vα-1** in Fig. 3).
2. In ternary systems, where a binary subsystem belong to type **2** complicated by a metastable immiscibility region, the three-phase immiscibility region can either remain metastable at any ratio B/C (see T-X* scheme **VIβ′-4** in Fig. 3), end in metastable conditions in the TCP (see T-X* schemes **IVα-2**, **IVβ-3** in Fig. 3), or transform into stable equilibria (see T-X* schemes **IIIβ-3**, **IIIβ-4**, **IIIβ-5**, **IVβ-5**, **Vε-5**, **VIβ-2**, **VIε-3** in Fig. 3).

If the immiscibility region ends in metastable conditions of the ternary system, the following transformation of quasi-binary sections from type **2a** into type **1a** takes place through the boundary version **12a** with the double critical end-point pQ (L = G–S) (see T-X* schemes **IVα-2**, **IVβ-3** in Fig. 3).

Transition of a three-phase immiscibility region of types **2d′** or **2c′** from metastable into stable equilibria takes place in a range of concentration of the second nonvolatile component that is added to the binary mixture of type **2d′** or **2c′**. The transition starts from high-temperature equilibria [point pR (L_1 = G–L_2–S)] at the lowest concentration of the second nonvolatile component and terminates in the low-temperature point NL ($L_1 = L_2$–G–S) at the highest concentration of the second nonvolatile component (see T-X* schemes **IIIβ-3**, **IIIβ-4**, **VIε-3** in Fig. 3). Such phase behavior was observed in the systems K_2SO_4–$KLiSO_4$–H_2O [34], SiO_2–$Na_2Si_2O_5$–H_2O [33], and Na_3PO_4–Na_2HPO_4–H_2O [35].

Another phase behavior occurs in the case of binary subsystems of types **2d″** or **2c″** where the low-temperature part of immiscibility region is stable already in the binary subsystems and the high-temperature part of immiscibility region undergoes transition from metastable into stable conditions in the ternary system (see T-X* schemes **IVα-2**, **IIIβ-5**, **IVβ-5**, **VIβ-2** in Fig. 3). Transition of three-phase immiscibility region into stable equilibria with an increasing concentration of the second nonvolatile component is terminated by an appearance of the ternary nonvariant points pR (L_1 = G–L_2–S). Simultaneously, the high-pressure critical curves $L_1 = L_2$–S, originated in the binary critical end-points Q and M, are coming close together as the concentration of the second nonvolatile component is

increasing and coincide in a DCEP MQ ($L_1 = L_2$–S). It can be shown that a DCEP MQ appears at a lower concentration of the second nonvolatile component in ternary mixture than in the case of an appearance of nonvariant critical point pR.

ACKNOWLEDGMENTS

The author would like to thank Dr. L. Z. Boshkov for careful reading of the first version of this manuscript and constructive comments, Dr. L. V. Yelash for helpful discussions, and Prof. D. G. Shaw for kind assistance in editing the manuscript and useful advice. Financial support by the Russian Fondues of Basic Research under Grant No 01-03-32770, as well as the CRDF (Grant RC1-2210) and INTAS (Grant 00-640) is gratefully acknowledged.

REFERENCES

1. J. D. van der Waals and Ph. Kohnstamm. *Lehrbuch der Termodynamik*, Barth, Leipzig (1912).
2. B. H. W. Roozeboom. *Z. Phys. Chem*. **30**, 385–429 (1899).
3. G. Tamman. *Lehrbuch der Heterogenen Gleichgewichte*, Braunschweig, Druck und Verlag von Fr. Vieweg und Sohn, A.-G. (1924).
4. R. L. Scott and P. N. van Konynenburg. *Faraday Discuss. Chem. Soc*. **49**, 87–97 (1970).
5. L. Z. Boshkov. *Dokl. Akad. Nauk SSSR* **294**, 901–905 (1987).
6. U. K. Deiters and I. L. Pegg. *J. Chem. Phys*. **90**, 6632–6641 (1989).
7. T. Kraska and U. K. Deiters. *J. Chem. Phys*. **96**, 539–547 (1992).
8. L. V. Yelash and Th. Kraska. *Ber. Bunsen. Phys. Chem*. **102**, 213–223 (1998).
9. L. V. Yelash and Th. Kraska. *Phys. Chem. Chem. Phys*. **1**, 307–311 (1999).
10. A. van Pelt, C. J. Peters, J. de Swaan Arons. *J. Chem. Phys*. **95**, 7569–7575 (1991).
11. A. H. Harvey. *J. Chem. Phys*. **95**, 479–484 (1991).
12. R. Thiery, S. N. Lvov, J. Dubessy. *J. Chem. Phys*. **109**, 214–222 (1998).
13. G. M. Schneider. *Advances Chem. Phys*. **17**, 1–42 (1970).
14. G. M.Schneider. In *Chemical Thermodinamics,* Vol. 2, pp. 105–146, The Chemical Society, London (1978).
15. V. M. Valyashko. *Phase Equilibria and Properties of Hydrothermal Systems* (Russian), Nauka, Moscow (1990).
16. V. M. Valyashko. *Pure Appl. Chem*. **62**, 2129–2138 (1990).
17. E. J. Ricci. *The Phase Rule and Heterogeneous Equilibria*, Van Nostrand, New York (1951).
18. G. W. Morey and W. T. Chen. *J. Chem. Soc*. **78**, 4249–4252 (1956).
19. M. I. Ravich. *Water-Salt Systems at Elevated Temperatures and Pressures* (Russian), Nauka, Moscow (1974).
20. W. B. Street. In *Chemical Engineering at Supercritical Fluid Conditions,* M. E. Paulaitis, J. M. L. Penninger, P. Davidson (Eds.), pp. 3–30, Ann Arbor Science, Ann Arbor, MI (1983).
21. M. E. Paulaitis, M. A. McHugh, C. P. Chai. *Chemical Engineering at Supercritical Fluid Conditions,* M. E. Paulaitis, J. M. L. Penninger, P. Davidson (Eds.), pp. 139–158, Ann Arbor Science, Ann Arbor (1983).
22. W. Poot and Th. W. de Loos. In *Abstracts of the 14th Symposium on Thermophysical Properties,* 25–30 June 2001, W. M. Hynes and B. A. Stevenson (Eds.), p. 460, NIST, Boulder, CO (2001).
23. A. Benrath, F. Gjedebo, B. Schiffers, *Z. Anorg. Allg. Chem*. **231**, 285–297 (1937).
24. V. M. Valyashko and M. A. Urusova. *Russ. J. Inorg. Chem*. **41**, 1297–1310 (1996).
25. W. L. Marshall and J. S. Gill. *J. Inorg. Nucl. Chem*. **25**, 1033–1041 (1963).
26. W. L. Marshall and J. S. Gill. *J. Inorg. Nucl. Chem*. **36**, 2303–2312 (1974).
27. V. M. Valyashko and M. A. Urusova. *Russ. J. Inorg. Chem*. **41**, 1297–1310 (1996).
28. W. L. Marshall, J. S. Gill, C. H. Secoy. *J. Amer. Chem. Soc*. **76**, 4279–4281(1954).

29. V. M. Valyashko. *Phys. Chem. Chem. Phys*. **4**, 1178–1189 (2002).
30. G. M. Schneider. *Pure Appl. Chem*. **65**, 173–182 (1993).
31. M. Bluma and U. K. Deiters. *Phys.Chem. Chem. Phys.* **1**, 4307–4313 (1999).
32. C. J. Peters and K. Gauter. *Chem. Rev.* **99**, 419–431 (1999).
33. V. M. Valyashko and K. G. Kravchuk. *Dokl. Akad. Nauk SSSR*. **242**, 1104–1107 (1978).
34. M. I. Ravich and V. M. Valyashko. *Zh. Neorgan. Khimii*. **14**, 1650–1654 (1969).
35. M. A. Urusova and V. M. Valyashko. *Zh. Neorgan. Khimii.* **46**, 866–872, 873–879 (2001).